HHS Public Access

Author manuscript

Sci Signal. Author manuscript; available in PMC 2022 March 21.

Published in final edited form as:

Sci Signal. 2021 September 21; 14(701): eabe0161. doi:10.1126/scisignal.abe0161.

Dissecting the biology of mTORC1 beyond rapamycin

Guang Yang[1,†,*], **Deanne Francis**[1,†,‡], **James R. Krycer**[1,‡], **Mark Larance**[1], **Ziyang Zhang**[3], **Chris J. Novotny**[3,‡], **Alexis Diaz-Vegas**[1], **Kevan M. Shokat**[3], **David E. James**[1,2,*]

[1]The University of Sydney, School of life and Environmental Sciences, The Charles Perkins Centre, Sydney, New South Wales, 2006, Australia.

[2]The University of Sydney, Sydney Medical School, New South Wales, 2006, Australia.

[3]Cellular and Molecular Pharmacology, Howard Hughes Medical Institute, University of California, San Francisco, 600 16th Street, San Francisco, CA, 94143, USA.

Abstract

Rapamycin extends maximal lifespan and increases resistance to starvation in many organisms. The beneficial effects of rapamycin are thought to be mediated by its inhibitory effects on the mechanistic target of rapamycin complex 1 (mTORC1), although it only partially inhibits the kinase activity of mTORC1. Other mTOR kinase inhibitors have been developed, such as Torin-1, but these readily cross react with mTORC2. Here, we report the distinct characteristics of a third generation mTOR inhibitor called RapaLink1. We found that low doses of RapaLink1 inhibited the phosphorylation of all mTORC1 substrates tested, including those whose phosphorylation is sensitive or resistant to inhibition by rapamycin, without affecting mTORC2 activity even after prolonged treatment. Compared with rapamycin, RapaLink1 showed better efficacy for inhibiting mTORC1 and potently blocked cell proliferation and induced autophagy. Moreover, using RapaLink1, we demonstrated that mTORC1 and mTORC2 exerted differential effects on cell glycolysis and glucose uptake. Finally, we found that RapaLink1 and rapamycin had opposing effects on starvation resistance in *Drosophila*. Consistent with the effects of RapaLink1, genetic blockade of mTORC1 activity made flies more sensitive to starvation, reflecting the complexity

[*]To whom correspondence may be addressed. guang.yang@sydney.edu.au; david.james@sydney.edu.au.

[‡]Current address:

D.F.: College of Public Health, Medical and Veterinary Sciences, Division of Tropical Health and Medicine Department of Biomedicine and Molecular and Cell Biology, James Cook University, Australia

J.R.K.: QIMR Berghofer Medical Research Institute, Brisbane, QLD 4006, Australia.

C.J.N.: Merck Research Laboratories, 213 E Grand Ave., South San Francisco, CA 94080, USA

[†]These authors contributed equally to this work.

Author contributions: G.Y. designed the experiments, performed molecular biology and all cell experiments, analysed the data, wrote the manuscript and supervised the work. D.F. designed the experiments, performed *Drosophila* experiments, analysed the date, and wrote the manuscript. J.R.K. performed measurement of lactate production and wrote the manuscript. M.L. performed size-exclusion chromatography. Z.Z., C.J.N. and K.M.S. synthesized RapaLink1. A.D. analysed the data of colony formation. D.E.J. designed experiments, wrote the manuscript, and supervised the work.

Competing interests: K.M.S. is an inventor on patents (10,117,945 and 10,646,577) owned by UCSF covering RapaLink-1 which are licensed to Revolution Medicines. K.M.S. has consulting agreements for the following companies, which involve monetary and/or stock compensation: Revolution Medicines, Black Diamond Therapeutics, BridGene Biosciences, Denali Therapeutics, Dice Molecules, eFFECTOR Therapeutics, Erasca, Genentech/Roche, Janssen Pharmaceuticals, Kumquat Biosciences, Kura Oncology, Mitokinin, Type6 Therapeutics, Venthera, Wellspring Biosciences (Araxes Pharma), Turning Point, Ikena, Initial Therapeutics and BioTheryX. The other authors declare that they have no competing interests.

Data and materials availability: All data needed to evaluate the conclusions in the paper are present in the paper or the Supplementary Materials.

of the mTORC1 network that extends beyond effects that can be inhibited by rapamycin. These findings extend our understanding of mTOR biology and provide insights into some of the beneficial effects of rapamycin.

Introduction

The mechanistic (formerly known as ‘mammalian’) target of rapamycin (mTOR) is a critical regulator of many major cellular functions, including cell growth, proliferation, metabolism, and survival. Dysregulation of the mTOR pathway has been implicated in many human diseases such as diabetes, epilepsy, neurodegeneration, and cancer. mTOR serves as a catalytic subunit of two functionally distinct multi-protein complexes termed mTOR complex 1 (mTORC1) and mTOR complex 2 (mTORC2). These complexes perform different functions in cells. mTORC1 integrates extra- and intracellular signal inputs (amino acids, growth factors, stress and energy status) to control key biological processes that are required for cell growth and proliferation, whereas mTORC2 mainly participates in cell metabolism and survival by activating Akt, PKCα and SGK1 (1–3).

There has been great interest in establishing the unique biological functions of these different mTOR complexes. One approach has involved generation of cell lines or animal models in which specific components of either the mTORC1 or mTORC2 have been genetically deleted, usually either Raptor or Rictor/SIN1, the specific subunits of the mTORC1 and mTORC2, respectively (4–7). A major limitation of these approaches is that the chronic absence of proteins with essential biological functions can lead to adaptive responses that may or may not have physiological relevance. For instance, in mouse embryonic fibroblasts (MEFs) lacking SIN1 (4), there is loss of FOXO1/3a phosphorylation, but other Akt substrates (TSC2 and GSK3) are unaffected, although Ser^{474} phosphorylation of Akt is abolished. However, acute prevention of Ser^{474} phosphorylation using a chemical genetics approach influences Akt2 activity toward several substrates, including both FOXO1/3a and TSC2 (8), indicating the existence of a compensatory mechanism in chronic knockout experiments.

To circumvent these issues, researchers have devised mTOR-specific small molecule inhibitors that can be added acutely to cells or animals followed by dynamic monitoring of biological consequences. In the case of mTORC1, the drug rapamycin has been invaluable. The discovery of mTOR arose from characterisation of this natural compound and only mTORC1 is acutely sensitive to inhibition by rapamycin, leading to rapamycin’s use as an mTORC1 inhibitor in both fundamental and clinical research for almost 30 years (1). Rapamycin forms a complex with the 12kDa FK506-binding protein (FRBP12), which binds to a domain adjacent to the active site of the kinase mTOR and reduces access to the active site cleft (9). Although rapamycin has been invaluable for studying mTORC1 biology, rapamycin inhibits only some of the phosphorylation events mediated by mTORC1. Thus, given that much of our knowledge about mTORC1 specific functions stems from the use of rapamycin, the existence of rapamycin-resistant mTORC1 substrates presents a gap in our broader understanding of mTORC1-specific functions. More potent 2^{nd} generation inhibitors that bind to the ATP binding site of mTOR, like Torin-1, can block both rapamycin-sensitive

and -resistant mTORC1 substrates. However, these drugs also interact with mTORC2 even at low concentrations and so their specificity is somewhat limited.

The Shokat lab developed a 3rd generation mTOR inhibitor, RapaLink1, which links rapamycin to an ATP competitive mTOR inhibitor (MLN0128), enabling it to overcome resistance to existing first- and second-generation inhibitors (11). RapaLink1 is selective towards mTORC1 at lower doses in human glioblastoma cell lines (12), suggesting that it could be used as a tool to decipher different functions of mTORC1 and mTORC2. In the current study, we confirmed this notion and validated that RapaLink1 selectively inhibited mTORC1 activity but not mTORC2 at low concentrations, and this activity spanned rapamycin-sensitive and resistant substrates in different cell types. Taking advantage of this characteristic of RapaLink1, we used it to examine the role of mTORC1 and mTORC2 in regulating different biological processes. We also compared the effects of rapamycin and Rapalink1 on starvation resistance in flies and found that, in contrast to rapamycin, which enhanced starvation resistance, complete inhibition of mTORC1 using RapaLink1 adversely affected starvation resistance. These findings extend our understanding of mTOR biology and provide insights into some of the beneficial effects of rapamycin.

Results

RapaLink1 selectively and completely inhibits mTORC1 signalling.

Although rapamycin is the most widely used mTORC1 inhibitor, it blocks the ability of mTORC1 to phosphorylate certain substrates but not others. The ‘high affinity’ mTORC1 substrates, such as ULK1, are still phosphorylated in the presence of rapamycin, whereas the phosphorylation of the “low affinity” substrate S6K is blocked (10). This differential sensitivity is site specific and not protein specific because 4E-BP1 contains both rapamycin-sensitive (Ser^{65}) and rapamycin-resistant ($Thr^{37/46}$) sites ((10), Fig. 1A and fig. S1A). Rapamycin is highly specific for mTORC1 because it had no significant effect on the ability of mTORC2 to inhibit its bona fide substrate Akt and its downstream target NDRG1 at multiple doses of the drug (Fig. 1B and C). In contrast, Torin-1 significantly inhibited mTORC1 activity but also inhibited mTORC2 activity (fig. S1B).

In contrast to Torin-1, RapaLink1 showed considerable specificity for mTORC1 at low doses without any demonstrable effects on mTORC2 activity. At low doses (3 nM), RapaLink1 selectively and almost completely blocked mTORC1 activity in HEK-293E cells toward both rapamycin-sensitive (S6K Thr^{389} and 4E-BP1 Ser^{65}) and rapamycin-resistant (4E-BP1 $Thr^{37/46}$ and ULK1 Ser^{757}) sites without any demonstrable effect on mTORC2 targets (Akt Ser^{473} and NDRG1 Thr^{346}) (Fig. 1B and C). We were unable to detect similar specificity for Torin-1 at any dose tested (fig. S1B). At 10 nM, RapaLink1 inhibited both mTOR complexes. We observed similar patterns in HeLa cells and 3T3-L1 adipocytes, suggesting that RapaLink1 at low concentrations represents a specific tool for studying mTORC1 biology independently of effects on mTORC2 (fig. S1C–E). The dose response characteristics of RapaLink1 varied among different cell lines (for example, mTORC1/2 in HeLa cells were three times as sensitive to RapaLink1 compared to HEK-239E cells) and so it is crucial to perform dose analyses on a case-by-case basis.

Prolonged treatment with low dose RapaLink1 does not inhibit mTORC2 activity.

Prolonged (>24 h) rapamycin treatment inhibits mTORC2 activity by blocking the assembly of mTORC2 in certain cell types (13), which has been suggested as a cause for some of the adverse clinical effects of rapamycin. We next tested if RapaLink1 has similar properties. We used PC3 cells because they display inhibition of mTORC2 with long-term rapamycin treatment (13). PC3 cells were more sensitive to RapaLink1 than other cell types we tested (Fig. 2A and B). Chronic treatment with 0.3 nM RapaLink1 caused substantial inhibition of mTORC1 activity without affecting mTORC2 activity, indicating that prolonged low-dose RapaLink1 treatment inhibited only mTORC1 but not mTORC2. The specificity of chronic RapaLink1 treatment on mTORC2 activity was also observed in HEK293E cells (Fig. 2C and D) whereas rapamycin caused weak inhibition, as previously reported (13). These data demonstrate the utility of using multiple rapamycin and RapaLink1 doses to distinguish between rapamycin-resistant mTORC1, rapamycin-sensitive mTORC1 and mTORC2 substrates in multiple cell-types (Fig. 2E).

Different effects of mTOR complexes on biological processes are distinguished by RapaLink1.

Based on the dependence of cell growth/size on mTORC1 activity (18), we assessed the effect of rapamycin, RapaLink1 and Torin-1 on cell size. Low dose RapaLink1 (3 nM), which only inhibits mTORC1, and high dose RapaLink1 (10 nM) and Torin-1, which inhibit both mTORC1 and mTORC2, had comparable effects on cell size, indicating that mTORC2 activity is dispensable for cell growth/size (Fig. 3A) in HEK293E cells. Although chronic rapamycin treatment caused slight inhibition of mTORC2 in HEK293E cells (Fig. 2C and D), RapaLink1 (3 nM) and rapamycin reduced the size of cells to a similar extent (Fig. 3A), indicating mTORC1 regulates cell size mainly through rapamycin-sensitive substrates, most likely S6K. Although the mTORC1–4E-BPs/EIF4E axis has also been reported to contribute to cell size regulation (19), S6K is thought to be the major downstream effector of mTORC1-driven cell growth (20, 21). For example, Ohanna *et al.* reported that cell size in S6K1-deficient cells is decreased and resistant to rapamycin *(21)*, which is consistent with our data

We then assessed the effect of RapaLink1 on cell proliferation, which also depends on mTORC1 activity. Although rapamycin treatment resulted in a slight but significant inhibition of proliferation, this was less potent than the effect observed with RapaLink1 (Fig. 3B and fig. S2A), indicating both rapamycin-sensitive and rapamycin-resistant mTORC1 substrates are involved in the regulation of cell proliferation. Again, there was no significant difference between 1 nM rapamycin (mTORC1 inhibition only) and 3 nM RapaLink1 or Torin-1 (mTORC1/2 inhibition) (Fig. 3B and fig. S2B). These data are consistent with the concept that blockage of mTORC2 is dispensable for the anti-proliferative activity of mTOR inhibitors (12, 22). Furthermore, 1nM RapaLink1 resulted in a more substantial reduction in colony size in colony formation assays than rapamycin treatment (Fig. 3C). Although 3nM RapaLink1 and Torin-1 treatment led to a further reduction of colony size compared to 1nM RapaLink1, this effect was very mild (Fig. 3C), indicating mTORC1 is the main regulator of colony formation.

Another mTORC1-dependent function is autophagy. mTORC1 suppresses autophagy through phosphorylating several effectors that play key roles in both early and later stages of autophagy, including ULK1 (23–25), ATG13 (23–25), UVRAG (26), DAP1 (27) and ATG14 (28). Although the rapamycin sensitivity of some mTORC1 substrates, such as ULK1 and ATG13, is controversial (10, 29, 30), we found the phosphorylation of Ser^{757} in ULK1 was resistant to rapamycin in HEK293E cells (fig. S1A and Fig. 3D). Consistent with these signalling data, acute treatment with rapamycin (4 h) had only mild effects on autophagy, whereas RapaLink1 caused a marked increase in LC3-II accumulation (Fig. 3D), indicating that the acute regulation of autophagy by mTORC1 is mainly mediated by rapamycin-resistant substrates. Like cell growth and size, low dose RapaLink1 (3 nM) had identical effects to high dose RapaLink1 (10 nM), Torin-1 and serum starvation consistent with mTORC1, but not mTORC2, being a key coordinator of the anabolic and catabolic response to various environmental and physiological stresses (31).

We next assessed the impact of RapaLink1 on aerobic glycolysis which is reported to be regulated by both mTORC1 and mTORC2 (1, 2, 32). As expected, both rapamycin and low dose (3 nM) RapaLink1 suppressed lactate production in HEK293E cells, a major readout of aerobic glycolysis. High dose (10 nM) RapaLink1 and Torin-1 caused a further reduction of lactate production (Fig. 3E), indicating that unlike autophagy and cell growth, glycolysis is regulated by interplay between mTORC1 and mTORC2 activities.

Insulin plays a major role in regulating the acute uptake of glucose into adipocytes by stimulating the translocation of the glucose transporter GLUT4 to the plasma membrane and whereas mTORC2 has been implicated in this process (33, 34), the role of mTORC1 is controversial (35, 36). We re-evaluated the effect of acute inhibition of mTORC1 and mTORC2 in 3T3-L1 adipocytes using RapaLink1 (Fig. 3F). Insulin-induced glucose uptake was not impaired after acute treatment with rapamycin or with low dose (3 nM) RapaLink1. In contrast, high dose (10 or 20 nM) RapaLink1 substantially inhibited insulin-induced glucose uptake, indicating a major role for mTORC2, but not mTORC1, in acute insulin-regulated glucose uptake. These data demonstrate that mTORC1 and mTORC2 exert differential effects on various biological processes.

mTORC2 disruption increases the resistance of mTORC1 to RapaLink1.

A problem of targeting mTOR complexes with small molecules is that a pool of free Raptor not associated with mTORC1 (37) can act as a reservoir for further mTORC1 formation by freeing mTOR associated with mTORC2. This may contribute to the development of drug resistance. We wanted to determine if this mechanism limits the utility of RapaLink1 as a specific mTORC1 inhibitor. We utilised 4-hydrotamoxifen (4-OHT)-inducible rictor knockout MEFs (iRicKO) to provide a source of additional mTOR. In control (EtOH treated) MEFs, 1 nM RapaLink1 significantly inhibited the phosphorylation of several major mTORC1 substrates, which was further increased at 3 nM. However, in Rictor KO (4-OHT treated) MEFs, 1 nM RapaLink1 had no effect on the phosphorylation of 4EBP1 or ULK1 and the dose required to completely inhibit mTORC1 increased to 10 nM (Fig. 4A). Thus, disruption of mTORC2 reduced the sensitivity of mTORC1 to RapaLink1.

To further validate if the resistance to RapaLink1 in Rictor KO cells stems from increasing mTORC1 levels, we performed size-exclusion chromatography (SEC) to fractionate lysates from control and Rictor KO MEFs. In control MEFs, mTOR and Rictor eluted in high-molecular weight fractions (~1.1–1MDa), consistent with the molecular weight of mTOR complex dimers (38, 39). Unlike mTOR and Rictor, a substantial amount (39%, fraction 7–9) of Raptor (~150kDa) was found in lower molecular weight fractions (Fig. 4B and C), consistent with the molecular weight of Raptor monomers, suggesting that this was the 'free' Raptor pool. The ratio of 'free' Raptor dropped from 39% to 13% in Rictor KO MEFs. Because total levels of Raptor did not substantially change (fig. S3), the altered free Raptor reflected increasing mTORC1 levels in Rictor KO MEFs, which is consistent with our hypothesis.

A similar phenomenon was observed in inducible raptor knockout MEFs (iRapKO) (Fig. 3D). In control MEFs, 10 nM RapaLink1 was sufficient to block mTORC2 activity. However, in Raptor KO MEFs, Akt phosphorylated at Ser^{473} was still present even up to 100 nM RapaLink1. Unlike Raptor, there was no detectable 'free' Rictor in cells (Fig. 4B). Increased resistance of mTORC2 to RapaLink1 upon Raptor depletion is likely due to inhibition of the negative feedback loop mediated by IRS (14, 15) and Grb10 (16, 17). These data suggest that disruption of one mTOR complex increases the resistance of other mTOR complexes to RapaLink1.

Complete inhibition of TORC1 reduces starvation resistance in flies.

The selective inhibition of mTORC1 activation by RapaLink1 in cell-based systems prompted us to evaluate the effect of this compound on TORC1 activity and function in vivo using *Drosophila melanogaster*. To avoid developmental effects, adult flies were raised on standard food and then given food supplemented with rapamycin or RapaLink1 for three days. We observed a significant reduction in phosphorylated dS6K Thr^{398} after both rapamycin and RapaLink1 treatment, but neither of them inhibited the TORC2 substrate phosphorylated dAkt Ser^{505} (Fig. 5A). We next evaluated the effect of this compound on starvation resistance which has been reported to be increased by rapamycin (40). In contrast to rapamycin, RapaLink1 significantly shortened fly survival under starvation conditions (Fig. 5B).

Although the above data suggest that there are divergent effects of different classes of TORC1 substrates on starvation resistance we wanted to ensure that this effect of Rapalink1 did not involve cross reactivity with TORC2. Torin-1 inhibited both TORC1 and TORC2 in flies (Fig. 5C) and in contrast to Rapalink1, Torin-1 had only a slight inhibitory effect on starvation resistance (Fig. 5D). This result might reflect competing and divergent effects of TORC1 versus TORC2 on starvation resistance. Indeed, disruption of TORC2 by knocking down Rictor or SIN1, two of key components of TORC2, significantly increased starvation resistance (fig. S4A and S4B). These data suggest that inhibition of TORC1 reduced starvation resistance. To further confirm this finding, we next examined starvation resistance in a genetically perturbed model using Raptor RNAi knockdown flies. Raptor was knocked down when flies were maintained at 29°C, as confirmed by reduced phosphorylation of dS6K Thr^{398} (Fig. 5E). As expected, depletion of Raptor significantly reduced survival

under starvation conditions (Fig. 5F), demonstrating that complete inhibition of TORC1 reduces starvation resistance in flies, consistent with the effect of Rapalink1. Consistent with TORC1 inhibition, activation of TORC1 by overexpressing Rheb (fig. S4C) or knockdown of TSC1 (fig. S4D) accelerated mortality under starvation conditions. These results indicate that TORC1 activation needs to be regulated within a certain range. Both hypo- and hyper-activation have an adverse effect under nutritional stress.

Discussion

Elevated mTOR activity has been linked to multiple chronic diseases and directly contributes to the process of ageing (41), leading a major exploration of mTOR inhibitors for the treatment of various diseases and as an anti-ageing medication. Currently, the only compounds targeting the mTOR signalling pathway for clinical application have been rapamycin and rapamycin analogs (rapalogs) and direct mTOR kinase inhibitors (2nd generation inhibitors). However, treatment with rapamycin and rapalogs have only achieved modest effects in major solid tumors in the clinic (42) and produce negative side effects, including hyperglycemia, hyperlipidaemia, insulin resistance and hypertension (43, 44). The poor efficacy of this class of drug partially stems from incomplete mTORC1 inhibition (45, 46) and at least some of the detrimental metabolic changes result from indirect attenuation of mTORC2 signalling (47, 48). Although the 2nd generation inhibitors more potently inhibit mTOR activity, they tend to indiscriminately inhibit both mTORC1 and mTORC2, leading to undesirable side effects. Therefore, there is an urgent need for more specific mTORC1 inhibitors. The development of small-molecule inhibitors of mTORC1 have offered proof-of-concept evidence (49–51). Although these inhibitors overcome the disadvantages of rapamycin to varying degrees, they still have their own limitations. For example, Schreiber and colleagues identified a rapamycin analog with much greater selectivity for mTORC1 than rapamycin. However, this drug still had minimal effects on the rapamycin-resistant functions of mTORC1 as an FKBP12-dependent rapalog (49). Navitor Pharmaceuticals have developed two compounds that indirectly inhibit mTORC1 through targeting Rheb (50) and Glut1 (51). Although these two drugs can inhibit the full functions of mTORC1, they may cause side effects of an unknown nature because of affecting mTORC1-independent functions of Rheb (52) and Glut1.

The 3rd generation mTOR inhibitor RapaLink1 was initially designed to overcome resistance to existing first- and second-generation inhibitors, because it can interact with the FRB domain of mTOR by binding to FKBP12, and also to simultaneously bind the kinase domain of mTOR acting as an ATP-competitive inhibitor (11). In this study, we showed that at a low dose, RapaLink1 selectively and completely inhibited mTORC1 activity, including both rapamycin-sensitive and -resistant substrates (Fig. 1B and C). Rapalink1 had a more potent effect than rapamycin on several key pathways that are linked to human diseases and ageing including cell proliferation, autophagy, and glycolysis (Fig. 3B, 3D and 3E). Furthermore, unlike rapamycin, long-term treatment with low dose RapaLink1 did not inhibit mTORC2 either in cell lines (Fig. 2A–D) or in vivo (Fig. 5A, (12)). This advantage of RapaLink1 enhances its potential utility in the clinic.

At higher doses, RapaLink1 did inhibit mTORC2 (Fig. 1B) in different cell types but at variable effective doses (fig. S1C–E). This special characteristic makes RapaLink1 unique from any other mTOR inhibitors and to be a powerful experimental tool to delineate distinct functions of mTORC1 and mTORC2. Using RapaLink1, we determined that: (i) mTOR mainly regulated cell growth/size and autophagy through mTORC1; (ii) only mTORC2 acutely affected insulin-induced glucose uptake; (iii) and both complexes played roles in aerobic glycolysis (Fig. 3A, D, E and F. By comparing rapamycin and Rapalink1, we could discriminate between rapamycin-sensitive and rapamycin-resistant functions of mTORC1 (Fig. 2E). A phosphoproteomics analysis using rapamycin- or RapaLink1-treated cells will resolve the full repertoire of rapamycin-sensitive and rapamycin-resistant mTORC1 substrates. However, the sensitivity of different cell types to Rapalink1 varied considerably (Fig. 1B, Fig. 2A–D and fig. S1B and C. In HEK293E cells, 3nM RapLink1 caused substantial inhibition of mTORC1 activity without affecting mTORC2 activity whereas in PC3 cells, the dose required to achieve the same effect was 10-fold less (0.3nM). Therefore, it is important to perform dose analyses before starting the experiments.

The narrow window between mTORC1 and mTORC2 inhibition is the major disadvantage of RapaLink1. In most cases, the selectivity for mTORC1 compared to mTORC2 inhibition is about 3-fold (Fig. 1B, Fig. 2A–D and fig. S1B and C). Therefore, the concentration of this drug needs to be chosen to selectively inhibit mTORC1. Although the narrow inhibition window may limit the application of RapaLink1 in vivo, the selectivity on TORC1 has been validated in both fly (Fig. 5A) and mouse, where 4mg/kg RapaLink1 inhibits the phosphorylation of S6 and 4EBP1, but not that of Akt Ser^{473} in multiple tissues (12). The mTORC1 selectivity of RapaLink1 in other model organisms or even humans need to be further investigated. Furthermore, chronic treatment of RapaLink1 still causes weight loss, glucose intolerance and liver toxicity in mice, similar to what was previously reported for rapamycin (53), indicating these side effects are likely to stem from inhibition of rapamycin-sensitive substrates. We further observed that disruption of one mTOR complex reduced the sensitivity of the other complex to RapaLink1 through different mechanisms (Fig. 4A and D. This phenomenon likely underpins the cell type-specificity of dose response effects of Rapalink1 (fig. S1C–E) in that different cell types may express different amounts of these two mTOR complexes.

The most exciting but surprising finding was that RapaLink1 had opposing effects on starvation resistance compared to Rapamycin in flies (Fig. 5A). Although we were unable to evaluate the effects of RapaLink1 on rapamycin-resistant substrates in flies due to lack of suitable antibodies, a previous study demonstrated that RapaLink1 substantially reduced phosphorylation of 4EBP1 $Thr^{37/46}$ in multiple mouse tissues (12). Consistent with this finding, we also showed that RapaLink1 inhibited phosphorylation of both rapamycin-sensitive and -resistant mTORC1 substrates at the same concentration in multiple cell-types. Therefore, we are confident that it could completely inhibit TORC1 in flies. Our further validation using Torin-1 and Raptor RNAi flies confirmed that depletion of TORC1 activity shortened rather than extended survival under starvation conditions (Fig. 5B and C). These unexpected findings could explain some controversial results from previous studies. For example, rapamycin has life extending properties and promotes starvation resistance in multiple model organisms (40). However, TOR (dTOR) mutant flies, where both mTORC1

and mTORC2 functions are impaired, show extended lifespan without effects on starvation resistance (54). Based on our work, we predict this reflects opposing effects of mTORC1 and mTORC2 on starvation resistance such that when both are disrupted simultaneously, the outcome will be determined by the aggregate contribution of the two competing pathways.

The beneficial effects of rapamycin on starvation resistance have been thought to stem from inhibition of TORC1-mediated protein synthesis or upregulation of autophagy. However, this may not be the case because constitutive activation of protein synthesis or blockage of autophagy overcomes the beneficial effects of rapamycin on lifespan but not on starvation resistance in flies (40). Another possibility is that rapamycin treatment affects fat metabolism and energy reserves, which may promote starvation resistance. Two groups have reported that rapamycin increases triglyceride stores (40, 55), an effect that is partially dependent on the activity of 4E-BP (55). Furthermore, 4E-BP can function as a metabolic brake during starvation, because 4E-BP null flies burn fat quicker and die faster than control flies in periods of starvation (55). Intriguingly, Torin-1 treatment or Raptor depletion reduces the total levels of 4E-BP1 in human foreskin fibroblasts (56). These findings raise the possibility that the opposing effect of RapaLink1 on starvation resistance arises from decreasing the total levels of 4E-BP through the rapamycin-resistant function of TORC1. Further experiments need to be performed to validate this hypothesis. In summary, mTORC1 has multiple targets. Inhibiting some of them (rapamycin targets) promotes starvation resistance whereas inhibiting all of them (RapaLink1 targets) impairs starvation resistance. This calls for a re-evaluation of the field with particular attention to the role of these different classes of mTORC1 dependent substrates.

Materials and Methods

Reagents and antibodies

Dulbecco's modified Eagle medium (DMEM) and L-GlutaMAX were from Gibco. Fetal bovine serum (FBS) was from Hyclone Laboratories. Insulin, DMSO, and Chloroquine were from Sigma-Aldrich. Rapamycin was from LC-laboratories. Torin-1 was from Tocris Bioscience. RapaLink1 was provided by Prof. Kevan Shokat. All primary antibodies were diluted 1:1000 in dilution buffer containing 5% BSA- 0.1% Tween 20 – 0.02% NaN3 in TBS buffer (1.2% Tris-HCl pH 7.4, 8.7% NaCl). Pan 14–3-3 polyclonal rabbit antibodies were from Santa Cruz Biotechnology. All other primary antibodies were from Cell Signalling Technology. The anti-mouse horseradish peroxidase (HRP)-conjugated secondary antibody was from GE Healthcare (Buckinghamshire, United Kingdom), and the anti-rabbit HRP-conjugated secondary antibody was from Jackson ImmunoResearch. Polyvinylidene diflouride membrane was purchased from Millipore (Billerica, MA). In some cases, IR dye 700- or 800-conjugated secondary antibodies were used, and these were obtained from Rockland Immunochemicals.

Cell culture

HeLa, C2C12 and HEK293E cells were maintained in Dulbecco modified Eagle medium (DMEM, 4.5 g of glucose/liter) with 2 mM L-GlutaMAX and 10% FBS. iRapKO MEFs and iRicKO MEFs were cultured in DMEM with 10%FBS, 2mM L-GlutaMAX, Non-Essential

Amino Acids and 1mM sodium pyrophate. 4-Hydroxytamoxifen (4-OHT)-induction of Raptor or Rictor Knockout was performed as previously described (57). 3T3-L1 fibroblasts (a gift from Howard Green, Harvard Medical School) were grown in DMEM containing 10% FBS and 2 mM L-GlutaMAX in 10% CO2 at 37 °C. For differentiation into adipocytes, cells were grown to confluence, then treated with DMEM/FBS containing 4 μg/ml insulin, 0.25mM dexamethasone, 0.5mM 3-isobutyl-1-methylxanthine and 100 ng/ml d-biotin. After 72 h, the differentiation medium was replaced with fresh FBS/DMEM containing 4 μg/ml insulin and 100 ng/ml d-biotin for a further 3 days, then replaced with fresh FBS/DMEM. Adipocytes were re-fed with FBS/DMEM every 48 h and utilized for experiments between 9 and 12 days after the initiation of differentiation. These cells were routinely tested for mycoplasma.

Western Blotting

Proteins were separated by SDS-PAGE and transferred to PVDF membranes. The membranes were incubated in a blocking buffer containing 5% skim milk in Tris-buffered saline (TBS) and immunoblotted with the relevant antibodies overnight at 4°C in the blocking buffer containing 5% BSA–0.1% Tween in TBS buffer. After incubation, the membranes were washed and incubated with HRP-labeled secondary antibodies for 1 hour and then detected by SuperSignal West Pico chemiluminescent substrate. In some cases, IR dye 700- or 800-conjugated secondary antibodies were used and then scanned at the 700- and 800-nm channels using an Odyssey IR imager.

Colony formation assay

HeLa cells were seeded into 6-well plates (300 cells/well) and left for 8–12 days until formation of visible colonies. Colonies were washed with PBS and fixed with 10% acetic acid/10% methanol for 20 minutes, then stained with 0.4% crystal violet in 20% ethanol for 20 minutes. After staining, the plates were washed and air-dried, and colony numbers were counted. Average size of colonies was measured using ImageJ. Briefly, colonies in each well were identified using the Trainable Weka Segmentation tool (58). After segmentation, images were transformed to 8-bit greyscale, followed by applying a threshold for each well individually and colony analysis. Plating efficiency (PE) in untreated cells was 0.46 (PE = N of colonies / N of cells plated). The area and number of colonies were normalised against untreated cells.

Hoechst assay

The Hoechst assays for cell proliferation were performed as described previously (59). Briefly, HeLa cells were seeded into 96-well plates (3,000 cells/well) and fed overnight in DMEM containing 10% FBS and 2 mM GlutaMAX. Cells were then treated with DMSO, 100 nM rapamycin, 1 or 3 nM RapaLink1 for 2 days. Media was aspirated, and the plate was frozen at −80 °C. Plates were then thawed at room temperature and 100 μL of water was added per well before freezing once more at −80 °C. Plates were thawed, followed by the addition of 100 μL Hoechst-33258 solution, containing 10 μg/mL Hoechst-33258 in TNE buffer (10mM Tris-HCl, pH 7.4, 2M NaCl, 1mM EDTA). The fluorescence was measured at FEx = 360 nm and FEm = 440 nm.

Cell size determinations

HEK-293E cells were treated with DMSO, 100nM Rapamycin, 100nM Torin-1 and RapaLink1 (3 and 10nM) for 24 hrs. To measure cell size, cells were harvested by trypsinization and diluted in PBS, and then 5,000–25,000 cells were subjected to cell size analysis on Countess™ II (Thermofisher).

Measurement of lactate production

Media lactate levels were assayed enzymatically as described previously (60). Briefly, the assay buffer was 1 M glycine, pH 9.2, 0.4 M hydrazine sulfate in 1 M NaOH, and 2.5 mM EDTA, adjusted to pH 9.2 with NaOH prior to the addition of 4 mM NAD+ and 2 units/ml lactate dehydrogenase (Roche Applied Science). An aliquot of medium sample was diluted in water (100 μl total) and incubated with 100 μl of assay buffer in a microplate format. Reactions were protected from light and incubated at room temperature for at least 1 h, after which the absorbance of NADH was measured at 340 nm. Reactions with medium samples without lactate dehydrogenase were included as a negative control. Lactate levels were quantified using a standard curve of lactate, added to the naive culture medium.

2-Deoxyglucose uptake assays

Following 4 hr serum-starvation in DMEM/0.2% BSA/1% GlutaMAX with DMSO or inhibitiors (100nM rapamycin, 3nM, 10nM and 20nM RapaLink1), cells were washed and incubated in pre-warmed Krebs–Ringer phosphate buffer containing 0.2% bovine serum albumin (BSA, Bovostar, Bovogen) (KRP buffer; 0.6 mM Na2HPO4, 0.4 mM NaH2PO4, 120 mM NaCl, 6 mM KCl, 1 mM CaCl2, 1.2 mM MgSO4 and 12.5 mM Hepes (pH 7.4)). Cells were stimulated with 100 nM insulin for 20 min. To determine non-specific glucose uptake, 25 μM cytochalasin B (ethanol, Sigma Aldrich) was added to the wells before addition of 2-[3H]deoxyglucose (2-DOG) (PerkinElmer). During the final 5 min 2-DOG (0.25 μCi, 50 μM) was added to cells to measure steady-state rates of 2DOG uptake. Following three washes with ice-cold PBS, cells were solubilised in PBS containing 1% (v/v) Triton X-100. Tracer uptake was quantified by liquid scintillation counting and data normalised for protein content. Data were further normalised to maximal insulin stimulation of control cells, set to 100%.

Size-exclusion chromatography

iRicKO MEFs treated with EtOH or 4-OHT were lysed in ice-cold CHAPS-containing buffer (50 mM Na-HEPES, 100 mM NaCl, 2 mM $MgCl_2$, 2 mM DTT, and 0.3% CHAPS, complete EDTA-free protease inhibitors). The lysate was passaged 6 times on ice through a 1 ml syringe with a 22-gauge and 27-gauge needle and cleared by ultracentrifugation at 12,000 × g for 20 min at 4°C. The cleared lysates were normalized to a protein concentration of 4 mg/mL in the CHAPS buffer. The lysates (500 uL per sample) were filtered to remove large particles through 0.45 μm spin filters (Millipore Ultrafree-MC) at 12,000 × g for 1 min at 4°C. Using a Thermo Dionex BioRS UHPLC system each sample kept at 4°C was injected (350 uL per sample) onto an Agilent AdvanceBio SEC column (7.8×300 mm, 300A pores, 2.7 um particles). Prior to separations the column was cooled to 5°C and pre-equilibrated with 10 column volumes of SEC running buffer (0.3% CHAPS, 50 mM

Na-HEPES, 100 mM NaCl, 2 mM $MgCl_2$, 2 mM DTT). The flow rate was 0.5 mL/min and 12 fractions were collected from retention time 8.5 to 14.5 min with a total run time per sample of 45 min. The fractions in the SEC running buffer were diluted into SDS-PAGE sample buffer and equal fraction volumes loaded for western blotting.

Drosophila stocks and procedures

The following stocks were obtained from the Bloomington *Drosophila* stock center (Indiana University, Indiana, USA): UAS-Rheb (#9688), UAS-Raptor RNAi HMS02306 (#41912), UAS-Rictor RNAi (HMS01588, # 36699), UAS-SIN1 RNAi (HMS01565, #36677), UAS-TSC1 RNAi (JF01484, #31039), TRIP RNAi control stocks (# 36306 and #3607), and *ubiquitous*-GAL4 (# 32551). The following flies were also used: W^{1118} (Vienna *Drosophila* Resource Centre, Vienna, Austria, #6000), UAS-mouseCD8::GFP (Kyoto Stock Center, Kyoto, Japan, #108068), *tubulin*-GAL80ts;*tubulin*-GAL4 (gift of Dr Essi Havula, University of Sydney). Flies were maintained at standard temperature, humidity and 12h light/dark cycle, unless otherwise stated. Flies were fed a standard diet of yeast and sugar.

The GAL4-UAS system was used for overexpression and knockdown experiments. Twenty *ubi*-GAL4 virgin females were crossed with 5 to 10 males carrying a UAS-RNAi, control or UAS-overexpression for three days. Newly emerged adult progeny with the correct genotype were mated for 48 hours and females were selected for experiments.

For temperature sensitive experiments, *tub*-$GAL80^{ts}$; *tub*-Gal4 females were crossed with UAS-Raptor RNAi 41912 males at 18 degrees for 5 days to ensure embryo survival. Flies were raised at 18ºC to repress the expression of *tub*-GAL4 and RNAi expression. Mated adult females were collected and placed into 29 degrees for three days to inactivate *tub*-$Gal80^{ts}$ and activate *tub*-GAL4 and RNAi expression. Females were then removed from 29ºC for western blotting or starvation resistance assays.

Drugs were administered into the fly food (2.5% sugar, 5% yeast, 1% Agar). Briefly, sugar and yeast were added to boiled agar on a hot plate and left to cool to 55C with stirring. 2mL of fly food was added into individual vials where stock solutions of Rapamycin, RapaLink1 and Torin-1 were diluted into cooled fly food (at 55ºC) for a final concentration of 200uM, 6uM and 10uM respectively. The same volume of ethanol was added as a vehicle control. Groups of 16 mated female flies were added to each vial for three days. Flies were then collected for western blotting or assayed for starvation resistance.

We used the Drosophila activity monitoring system (Trikinetics) (61) to assay survival during starvation. Sixteen mated female flies were placed into individual DAMs tubes sealed with 2% agar on one end and a cotton plug on the other end. Monitors were kept in 25ºC/65% humidity with 12hour Light/Dark cycles for all experiments. Activity was monitored every 5 minutes and death was counted as a complete absence of activity lasting longer than 5 minutes. The median starvation resistance was derived with the survival and survminor packages (R).

To prepare samples for Western blotting, mated adult female flies were anesthetised with CO2. A scalpel was used to quickly separate the head and thorax from the abdomen. Heads and thoraxes were then flash frozen in liquid N_2.

Supplementary Material

Refer to Web version on PubMed Central for supplementary material.

Acknowledgements:

We thank Prof. Michael Hall for providing iRapKO and iRicKO MEF cells.

Funding:

This work was supported by National Health and Medical Research Council (NHMRC) project grant (GNT1120201) and National Institutes of Health (NIH) grant (1R01CA221969). K.M.S. was supported by the Samuel Waxman Research Foundation. J.R.K. was supported by an Australian Diabetes Society Skip Martin Early-Career Fellowship. M.L. is a Cancer Institute NSW Future Research Leader Fellow. Z.Z. is a Damon Runyon Fellow supported by the Damon Runyon Cancer Research Foundation (DRG-2281-17). D.E.J. is an NHMRC Senior Principal Research Fellow

References and Notes

1. Saxton RA, Sabatini DM, mTOR Signaling in Growth, Metabolism, and Disease. Cell 169, 361–371 (2017).
2. Ben-Sahra I, Manning BD, mTORC1 signaling and the metabolic control of cell growth. Curr Opin Cell Biol 45, 72–82 (2017). [PubMed: 28411448]
3. Zhu Z, Yang C, Iyaswamy A, Krishnamoorthi S, Sreenivasmurthy SG, Liu J, Wang Z, Tong BC, Song J, Lu J, Cheung KH, Li M, Balancing mTOR Signaling and Autophagy in the Treatment of Parkinson's Disease. International journal of molecular sciences 20, (2019).
4. Jacinto E, Facchinetti V, Liu D, Soto N, Wei S, Jung SY, Huang Q, Qin J, Su B, SIN1/MIP1 maintains rictor-mTOR complex integrity and regulates Akt phosphorylation and substrate specificity. Cell 127, 125–137 (2006). [PubMed: 16962653]
5. Kumar A, Lawrence JC Jr., Jung DY, Ko HJ, Keller SR, Kim JK, Magnuson MA, Harris TE, Fat cell-specific ablation of rictor in mice impairs insulin-regulated fat cell and whole-body glucose and lipid metabolism. Diabetes 59, 1397–1406 (2010). [PubMed: 20332342]
6. Bentzinger CF, Romanino K, Cloetta D, Lin S, Mascarenhas JB, Oliveri F, Xia J, Casanova E, Costa CF, Brink M, Zorzato F, Hall MN, Ruegg MA, Skeletal muscle-specific ablation of raptor, but not of rictor, causes metabolic changes and results in muscle dystrophy. Cell metabolism 8, 411–424 (2008). [PubMed: 19046572]
7. Lee PL, Tang Y, Li H, Guertin DA, Raptor/mTORC1 loss in adipocytes causes progressive lipodystrophy and fatty liver disease. Mol Metab 5, 422–432 (2016). [PubMed: 27257602]
8. Kearney AL, Cooke KC, Norris DM, Zadoorian A, Krycer JR, Fazakerley DJ, Burchfield JG, James DE, Serine 474 phosphorylation is essential for maximal Akt2 kinase activity in adipocytes. The Journal of biological chemistry 294, 16729–16739 (2019). [PubMed: 31548312]
9. Aylett CH, Sauer E, Imseng S, Boehringer D, Hall MN, Ban N, Maier T, Architecture of human mTOR complex 1. Science 351, 48–52 (2016). [PubMed: 26678875]
10. Kang SA, Pacold ME, Cervantes CL, Lim D, Lou HJ, Ottina K, Gray NS, Turk BE, Yaffe MB, Sabatini DM, mTORC1 phosphorylation sites encode their sensitivity to starvation and rapamycin. Science 341, 1236566 (2013). [PubMed: 23888043]
11. Rodrik-Outmezguine VS, Okaniwa M, Yao Z, Novotny CJ, McWhirter C, Banaji A, Won H, Wong W, Berger M, de Stanchina E, Barratt DG, Cosulich S, Klinowska T, Rosen N, Shokat KM, Overcoming mTOR resistance mutations with a new-generation mTOR inhibitor. Nature 534, 272–276 (2016). [PubMed: 27279227]

12. Fan Q, Aksoy O, Wong RA, Ilkhanizadeh S, Novotny CJ, Gustafson WC, Truong AY, Cayanan G, Simonds EF, Haas-Kogan D, Phillips JJ, Nicolaides T, Okaniwa M, Shokat KM, Weiss WA, A Kinase Inhibitor Targeted to mTORC1 Drives Regression in Glioblastoma. Cancer cell 31, 424–435 (2017). [PubMed: 28292440]
13. Sarbassov DD, Ali SM, Sengupta S, Sheen JH, Hsu PP, Bagley AF, Markhard AL, Sabatini DM, Prolonged rapamycin treatment inhibits mTORC2 assembly and Akt/PKB. Molecular cell 22, 159–168 (2006). [PubMed: 16603397]
14. Harrington LS, Findlay GM, Gray A, Tolkacheva T, Wigfield S, Rebholz H, Barnett J, Leslie NR, Cheng S, Shepherd PR, Gout I, Downes CP, Lamb RF, The TSC1–2 tumor suppressor controls insulin-PI3K signaling via regulation of IRS proteins. The Journal of cell biology 166, 213–223 (2004). [PubMed: 15249583]
15. Shah OJ, Wang Z, Hunter T, Inappropriate activation of the TSC/Rheb/mTOR/S6K cassette induces IRS1/2 depletion, insulin resistance, and cell survival deficiencies. Current biology : CB 14, 1650–1656 (2004). [PubMed: 15380067]
16. Yu Y, Yoon SO, Poulogiannis G, Yang Q, Ma XM, Villen J, Kubica N, Hoffman GR, Cantley LC, Gygi SP, Blenis J, Phosphoproteomic analysis identifies Grb10 as an mTORC1 substrate that negatively regulates insulin signaling. Science 332, 1322–1326 (2011). [PubMed: 21659605]
17. Hsu PP, Kang SA, Rameseder J, Zhang Y, Ottina KA, Lim D, Peterson TR, Choi Y, Gray NS, Yaffe MB, Marto JA, Sabatini DM, The mTOR-regulated phosphoproteome reveals a mechanism of mTORC1-mediated inhibition of growth factor signaling. Science 332, 1317–1322 (2011). [PubMed: 21659604]
18. Yoon MS, The Role of Mammalian Target of Rapamycin (mTOR) in Insulin Signaling. Nutrients 9, (2017).
19. Fingar DC, Salama S, Tsou C, Harlow E, Blenis J, Mammalian cell size is controlled by mTOR and its downstream targets S6K1 and 4EBP1/eIF4E. Genes & development 16, 1472–1487 (2002). [PubMed: 12080086]
20. Magnuson B, Ekim B, Fingar DC, Regulation and function of ribosomal protein S6 kinase (S6K) within mTOR signalling networks. The Biochemical journal 441, 1–21 (2012). [PubMed: 22168436]
21. Ohanna M, Sobering AK, Lapointe T, Lorenzo L, Praud C, Petroulakis E, Sonenberg N, Kelly PA, Sotiropoulos A, Pende M, Atrophy of S6K1 − / − skeletal muscle cells reveals distinct mTOR effectors for cell cycle and size control. Nat. Cell Biol. 7, 286–294 (2005). [PubMed: 15723049]
22. Atkin J, Halova L, Ferguson J, Hitchin JR, Lichawska-Cieslar A, Jordan AM, Pines J, Wellbrock C, Petersen J, Torin1-mediated TOR kinase inhibition reduces Wee1 levels and advances mitotic commitment in fission yeast and HeLa cells. Journal of cell science 127, 1346–1356 (2014). [PubMed: 24424027]
23. Ganley IG, Lam du H, Wang J, Ding X, Chen S, Jiang X, ULK1.ATG13.FIP200 complex mediates mTOR signaling and is essential for autophagy. The Journal of biological chemistry 284, 12297–12305 (2009). [PubMed: 19258318]
24. Hosokawa N, Hara T, Kaizuka T, Kishi C, Takamura A, Miura Y, Iemura S, Natsume T, Takehana K, Yamada N, Guan JL, Oshiro N, Mizushima N, Nutrient-dependent mTORC1 association with the ULK1-Atg13-FIP200 complex required for autophagy. Molecular biology of the cell 20, 1981–1991 (2009). [PubMed: 19211835]
25. Jung CH, Jun CB, Ro SH, Kim YM, Otto NM, Cao J, Kundu M, Kim DH, ULK-Atg13-FIP200 complexes mediate mTOR signaling to the autophagy machinery. Molecular biology of the cell 20, 1992–2003 (2009). [PubMed: 19225151]
26. Kim YM, Jung CH, Seo M, Kim EK, Park JM, Bae SS, Kim DH, mTORC1 Phosphorylates UVRAG to Negatively Regulate Autophagosome and Endosome Maturation. Molecular cell, (2014).
27. Koren I, Reem E, Kimchi A, DAP1, a novel substrate of mTOR, negatively regulates autophagy. Current biology : CB 20, 1093–1098 (2010). [PubMed: 20537536]
28. Yuan HX, Russell RC, Guan KL, Regulation of PIK3C3/VPS34 complexes by MTOR in nutrient stress-induced autophagy. Autophagy 9, 1983–1995 (2013). [PubMed: 24013218]

29. Puente C, Hendrickson RC, Jiang X, Nutrient-regulated Phosphorylation of ATG13 Inhibits Starvation-induced Autophagy. The Journal of biological chemistry 291, 6026–6035 (2016). [PubMed: 26801615]
30. Kim J, Kundu M, Viollet B, Guan KL, AMPK and mTOR regulate autophagy through direct phosphorylation of Ulk1. Nature cell biology 13, 132–141 (2011). [PubMed: 21258367]
31. Paquette M, El-Houjeiri L, Pause A, mTOR Pathways in Cancer and Autophagy. Cancers (Basel) 10, (2018).
32. Chi H, Sin1-mTORC2 signaling drives glycolysis of developing thymocytes. J Mol Cell Biol 11, 91–92 (2019). [PubMed: 30496428]
33. Kleinert M, Sylow L, Fazakerley DJ, Krycer JR, Thomas KC, Oxboll AJ, Jordy AB, Jensen TE, Yang G, Schjerling P, Kiens B, James DE, Ruegg MA, Richter EA, Acute mTOR inhibition induces insulin resistance and alters substrate utilization in vivo. Mol Metab 3, 630–641 (2014). [PubMed: 25161886]
34. Mao Z, Zhang W, Role of mTOR in Glucose and Lipid Metabolism. International journal of molecular sciences 19, (2018).
35. Pereira MJ, Palming J, Rizell M, Aureliano M, Carvalho E, Svensson MK, Eriksson JW, mTOR inhibition with rapamycin causes impaired insulin signalling and glucose uptake in human subcutaneous and omental adipocytes. Mol Cell Endocrinol 355, 96–105 (2012). [PubMed: 22333157]
36. Tremblay F, Gagnon A, Veilleux A, Sorisky A, Marette A, Activation of the mammalian target of rapamycin pathway acutely inhibits insulin signaling to Akt and glucose transport in 3T3-L1 and human adipocytes. Endocrinology 146, 1328–1337 (2005). [PubMed: 15576463]
37. Kim K, Qiang L, Hayden MS, Sparling DP, Purcell NH, Pajvani UB, mTORC1-independent Raptor prevents hepatic steatosis by stabilizing PHLPP2. Nat Commun 7, 10255 (2016). [PubMed: 26743335]
38. Yang H, Jiang X, Li B, Yang HJ, Miller M, Yang A, Dhar A, Pavletich NP, Mechanisms of mTORC1 activation by RHEB and inhibition by PRAS40. Nature 552, 368–373 (2017). [PubMed: 29236692]
39. Scaiola A, Mangia F, Imseng S, Boehringer D, Berneiser K, Shimobayashi M, Stuttfeld E, Hall MN, Ban N, Maier T, The 3.2-A resolution structure of human mTORC2. Sci Adv 6, (2020).
40. Bjedov I, Toivonen JM, Kerr F, Slack C, Jacobson J, Foley A, Partridge L, Mechanisms of life span extension by rapamycin in the fruit fly Drosophila melanogaster. Cell metabolism 11, 35–46 (2010). [PubMed: 20074526]
41. Johnson SC, Rabinovitch PS, Kaeberlein M, mTOR is a key modulator of ageing and age-related disease. Nature 493, 338–345 (2013). [PubMed: 23325216]
42. Li J, Kim SG, Blenis J, Rapamycin: one drug, many effects. Cell metabolism 19, 373–379 (2014). [PubMed: 24508508]
43. Johnston O, Rose CL, Webster AC, Gill JS, Sirolimus is associated with new-onset diabetes in kidney transplant recipients. Journal of the American Society of Nephrology : JASN 19, 1411–1418 (2008). [PubMed: 18385422]
44. Xie J, Wang X, Proud CG, mTOR inhibitors in cancer therapy. F1000Res 5, (2016).
45. Thoreen CC, Sabatini DM, Rapamycin inhibits mTORC1, but not completely. Autophagy 5, 725–726 (2009). [PubMed: 19395872]
46. Choo AY, Yoon SO, Kim SG, Roux PP, Blenis J, Rapamycin differentially inhibits S6Ks and 4E-BP1 to mediate cell-type-specific repression of mRNA translation. Proceedings of the National Academy of Sciences of the United States of America 105, 17414–17419 (2008). [PubMed: 18955708]
47. Barlow AD, Xie J, Moore CE, Campbell SC, Shaw JA, Nicholson ML, Herbert TP, Rapamycin toxicity in MIN6 cells and rat and human islets is mediated by the inhibition of mTOR complex 2 (mTORC2). Diabetologia 55, 1355–1365 (2012). [PubMed: 22314813]
48. Lamming DW, Ye L, Katajisto P, Goncalves MD, Saitoh M, Stevens DM, Davis JG, Salmon AB, Richardson A, Ahima RS, Guertin DA, Sabatini DM, Baur JA, Rapamycin-induced insulin resistance is mediated by mTORC2 loss and uncoupled from longevity. Science 335, 1638–1643 (2012). [PubMed: 22461615]

49. Schreiber KH, Arriola Apelo SI, Yu D, Brinkman JA, Velarde MC, Syed FA, Liao CY, Baar EL, Carbajal KA, Sherman DS, Ortiz D, Brunauer R, Yang SE, Tzannis ST, Kennedy BK, Lamming DW, A novel rapamycin analog is highly selective for mTORC1 in vivo. Nat Commun 10, 3194 (2019). [PubMed: 31324799]
50. Mahoney SJ, Narayan S, Molz L, Berstler LA, Kang SA, Vlasuk GP, Saiah E, A small molecule inhibitor of Rheb selectively targets mTORC1 signaling. Nat Commun 9, 548 (2018). [PubMed: 29416044]
51. Kang SA, O'Neill DJ, Machl AW, Lumpkin CJ, Galda SN, Sengupta S, Mahoney SJ, Howell JJ, Molz L, Hahm S, Vlasuk GP, Saiah E, Discovery of Small-Molecule Selective mTORC1 Inhibitors via Direct Inhibition of Glucose Transporters. Cell Chem Biol 26, 1203–1213 e1213 (2019). [PubMed: 31231029]
52. Lacher MD, Pincheira R, Zhu Z, Camoretti-Mercado B, Matli M, Warren RS, Castro AF, Rheb activates AMPK and reduces p27Kip1 levels in Tsc2-null cells via mTORC1-independent mechanisms: implications for cell proliferation and tumorigenesis. Oncogene 29, 6543–6556 (2010). [PubMed: 20818424]
53. Ehinger Y, Zhang Z, Phamluong K, Soneja D, Shokat KM, Ron D, Brain-specific inhibition of mTORC1 by a dual drug strategy: a novel approach for the treatment of alcohol use disorder. bioRxiv, (2020)
54. Luong N, Davies CR, Wessells RJ, Graham SM, King MT, Veech R, Bodmer R, Oldham SM, Activated FOXO-mediated insulin resistance is blocked by reduction of TOR activity. Cell metabolism 4, 133–142 (2006). [PubMed: 16890541]
55. Teleman AA, Chen YW, Cohen SM, 4E-BP functions as a metabolic brake used under stress conditions but not during normal growth. Genes & development 19, 1844–1848 (2005). [PubMed: 16103212]
56. Clippinger AJ, Maguire TG, Alwine JC, The changing role of mTOR kinase in the maintenance of protein synthesis during human cytomegalovirus infection. Journal of virology 85, 3930–3939 (2011). [PubMed: 21307192]
57. Cybulski N, Zinzalla V, Hall MN, Inducible raptor and rictor knockout mouse embryonic fibroblasts. Methods in molecular biology 821, 267–278 (2012). [PubMed: 22125071]
58. Arganda-Carreras I, Kaynig V, Rueden C, Eliceiri KW, Schindelin J, Cardona A, Seung HS, Trainable Weka Segmentation: a machine learning tool for microscopy pixel classification. Bioinformatics 33, 2424–2426 (2017). [PubMed: 28369169]
59. Krycer JR, Phan L, Brown AJ, A key regulator of cholesterol homoeostasis, SREBP-2, can be targeted in prostate cancer cells with natural products. The Biochemical journal 446, 191–201 (2012). [PubMed: 22657538]
60. Krycer JR, Quek LE, Francis D, Fazakerley DJ, Elkington SD, Diaz-Vegas A, Cooke KC, Weiss FC, Duan X, Kurdyukov S, Zhou PX, Tambar UK, Hirayama A, Ikeda S, Kamei Y, Soga T, Cooney GJ, James DE, Lactate production is a prioritized feature of adipocyte metabolism. The Journal of biological chemistry 295, 83–98 (2020). [PubMed: 31690627]
61. Pfeiffenberger C, Lear BC, Keegan KP, Allada R, Locomotor activity level monitoring using the Drosophila Activity Monitoring (DAM) System. Cold Spring Harb Protoc 2010, pdb prot5518 (2010). [PubMed: 21041391]

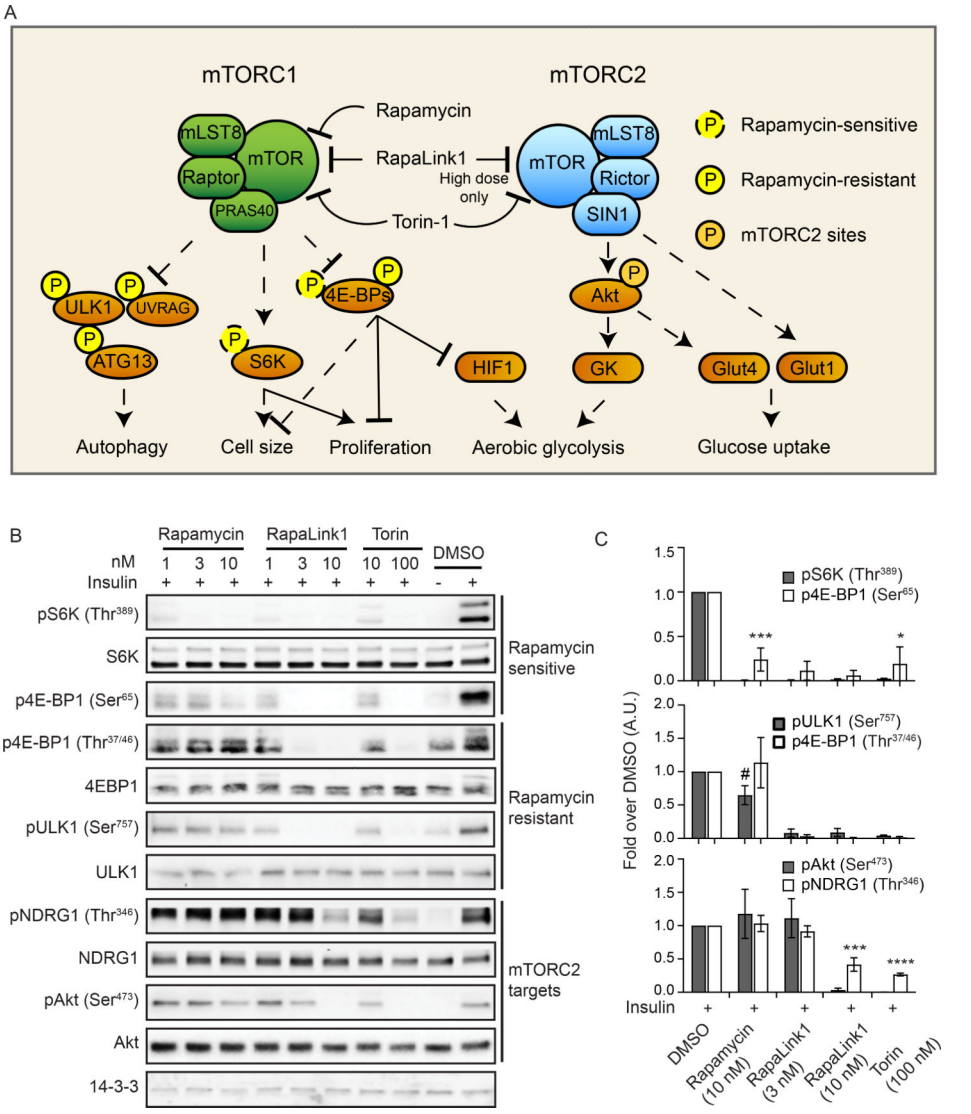

Fig. 1. RapaLink1 selectively and completely inhibits mTORC1 signalling at low doses.

(**A**) Schematic shows the mTOR signalling network. **(B)** Western blotting analysis for mTORC1 and mTORC2 substrates on lysates from HEK293E cells treated with Rapamycin, RapaLink1 and Torin-1 at the indicated doses for 4 hours under serum starvation, then stimulated with insulin (100 nM and 10 min). **(C)** Graph shows mean ± SEM of densitometry analyses of the Western blots in Fig. 1B normalized to total protein from 3 independent experiments. A.U., arbitrary units. * P<0.05, *** P<0.005, **** P<0.001, # No significant difference, two-tailed student's t test.

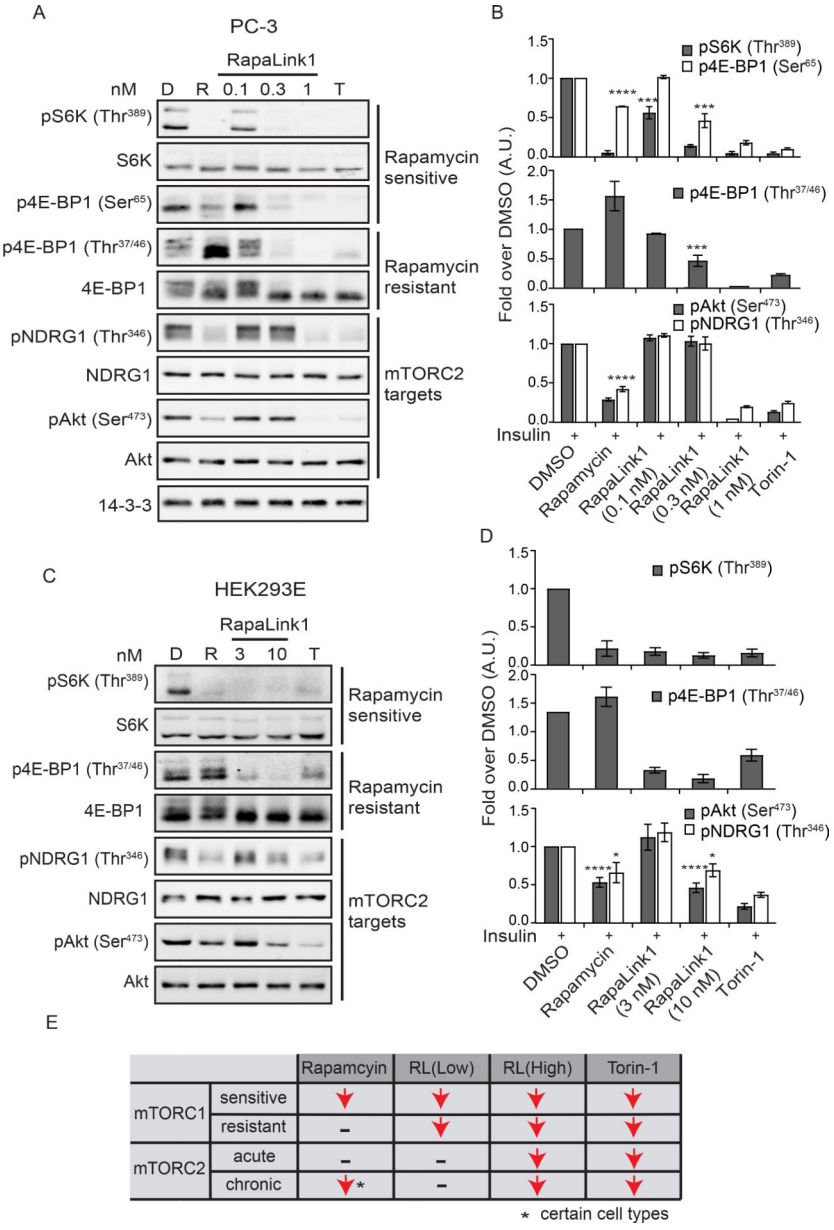

E

		Rapamcyin	RL(Low)	RL(High)	Torin-1
mTORC1	sensitive	↓	↓	↓	↓
	resistant	–	↓	↓	↓
mTORC2	acute	–	–	↓	↓
	chronic	↓*	–	↓	↓

* certain cell types

Fig. 2. Prolonged treatment of low dose RapaLink1 does not inhibit mTORC2 activity.

(A, C) Western blotting analysis for mTORC1 and mTORC2 substrates on lysates from PC3 (A) or HEK293E (C) cells treated with DMSO, rapamycin, Torin-1 and RapaLink1 at the indicated doses for 24 hrs. Blots are representative of 3 (A) or 4 (C) independent experiments. D, DMSO; R, rapamycin, T, Torin-1. **(B, D)** Graph shows mean ± SEM of densitometry analyses of the Western blots in Fig. 2A and 2C normalized to total protein from 3 (B) or 4 (D) independent experiments. A.U., arbitrary units. * P<0.05, *** P<0.005, **** P<0.001, two-tailed student's t test. **(E)** Summary of the effects of the three inhibitors on different mTOR substrates. RL, RapaLink1.

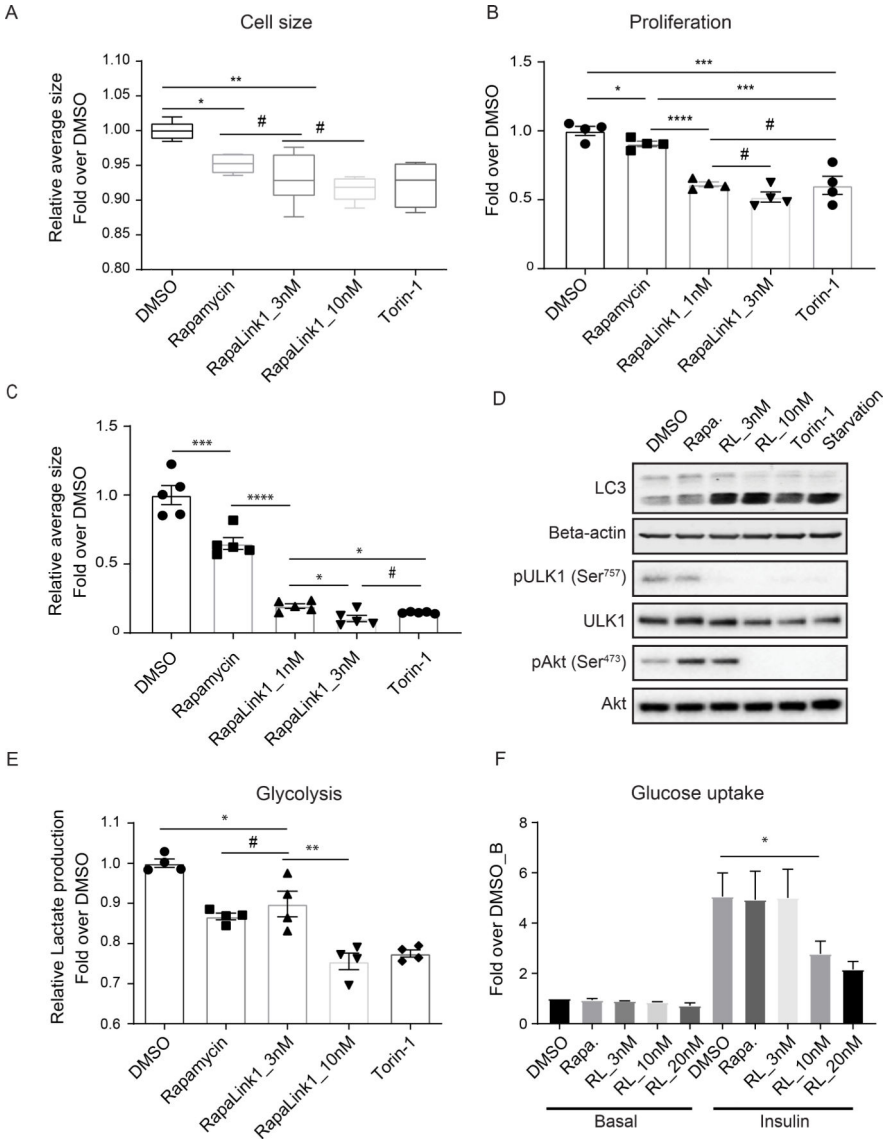

Fig. 3. Functional outcome of mTOR inhibition by RapaLink1.

(A) Cell size analysis of HEK293E cells treated with DMSO, 10nM Rapamycin, 100nM Torin-1 and RapaLink1 at the indicated doses for 24 h. Data are presented as mean ± SEM (* P<0.05, *** P<0.005, # No significant difference, two-tailed student's t test, n≥4 independent experiments). **(B)** Hoechst assay for cell proliferation in HeLa cells treated with DMSO, 100nM Rapamycin, RapaLink1 at the indicated doses or 100nM Torin-1 for 48 hrs. Data are presented as mean ± SEM from 4 independent experiments (*P<0.05, *** P<0.005, **** P<0.001, # No significant difference, two-tailed student's t test). **(C)** Colony formation assay performed in HeLa cells treated with DMSO, 100nM Rapamycin, RapaLink1 at the indicated doses or 100nM Torin-1 for 8 days. Data are presented as mean ± SEM from 5 independent experiments (*P<0.05, *** P<0.005, **** P<0.001, # No significant difference, two-tailed student's t test). **(D)** Western blotting analysis for LC3, beta-actin, total and phosphorylated ULK1 and Akt on lysates from HEK293E cells treated with DMSO, 100nM Rapamycin, 100nM Torin-1 and RapaLink1 at the indicated doses for 4 h or

serum starved for 4 h. Chloroquine (100μM) was added to medium 30 min prior to harvest. Blots are representative of 3 independent experiments. **(E)** Lactate production was assessed in HEK293E cells treated with DMSO, 100nM Rapamycin, 100nM Torin-1 and RapaLink1 at the indicated doses for 8 h. Data are presented as mean ± SEM from 4 independent experiments (*P<0.05, ** P<0.01, # No significant difference, two-tailed student's t test). **(F)** 2-[^{3}H] deoxyglucose uptake was quantified in 3T3-L1 adipocytes treated with DMSO, 100nM Rapamycin and RapaLink1 at the indicated doses for 4 hours under serum starvation, then stimulated with insulin (100 nM and 20 min). Data are presented as means ± SEM from 3 independent experiments (*P<0.05, two-tailed student's t test).

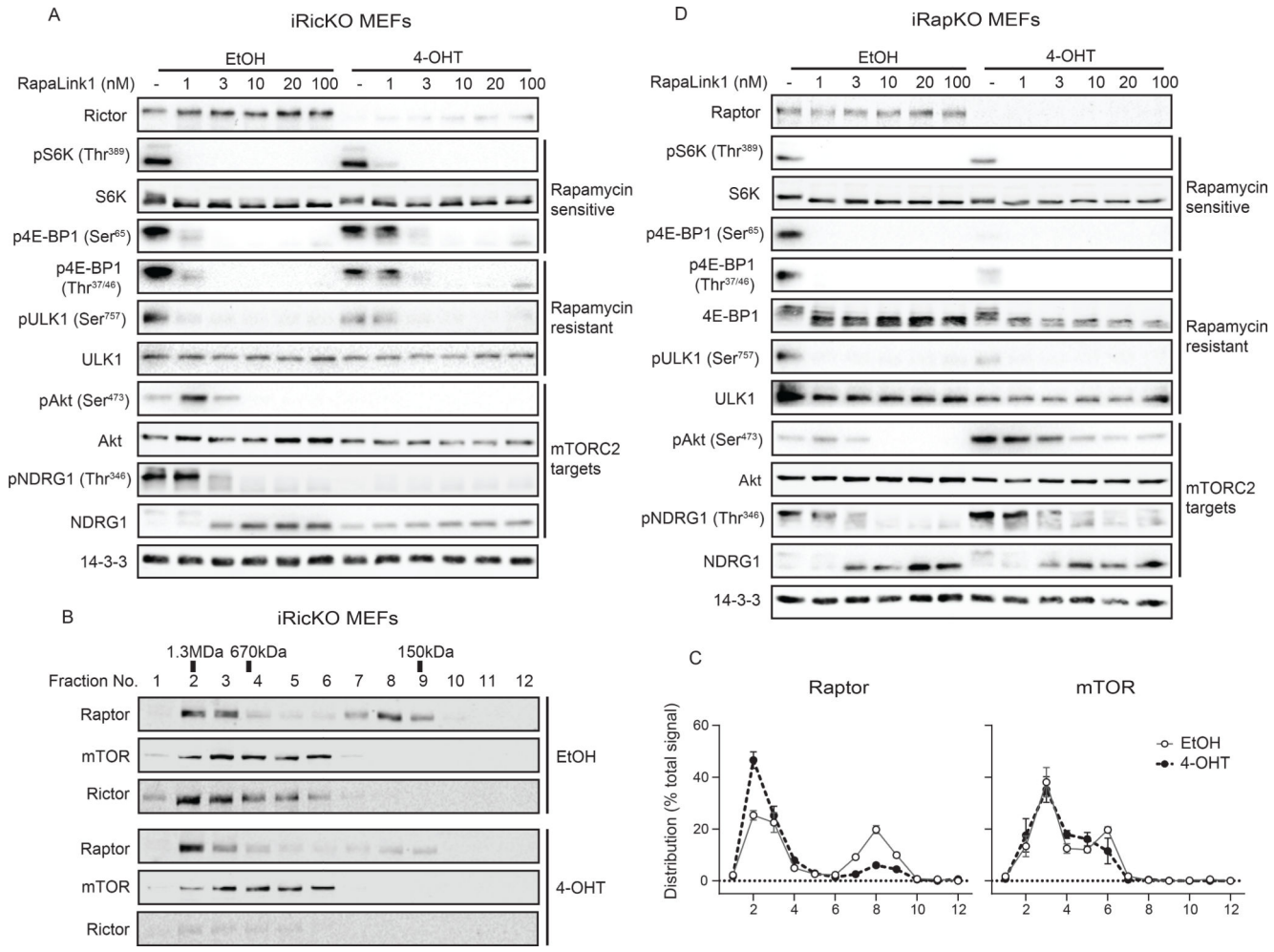

Fig. 4. Disruption of one mTOR complex increases the resistance of other mTOR complex to RapaLink1.

(A, D) Western blotting analysis for mTORC1 and mTORC2 substrates on lysates from iRicKO MEFs (A) or iRapKO MEFs (D) treated with ethanol or 1 mM 4-hydroxytamoxifen (4-OHT) for 3 d to induce Raptor or Rictor knockout. Treated cells were incubated with DMSO or RapaLink1 at the dose indicated for 4 h. Blots are representative of 3 independent experiments. **(B, C)** Western blotting analysis for raptor and mTOR on lysates from iRicKO MEFs treated with ethanol (EtOH) or 4-OHT, following size-exclusion chromatography (B) and quantification of signal per fraction, normalized to total protein (C) from 3 independent experiments.

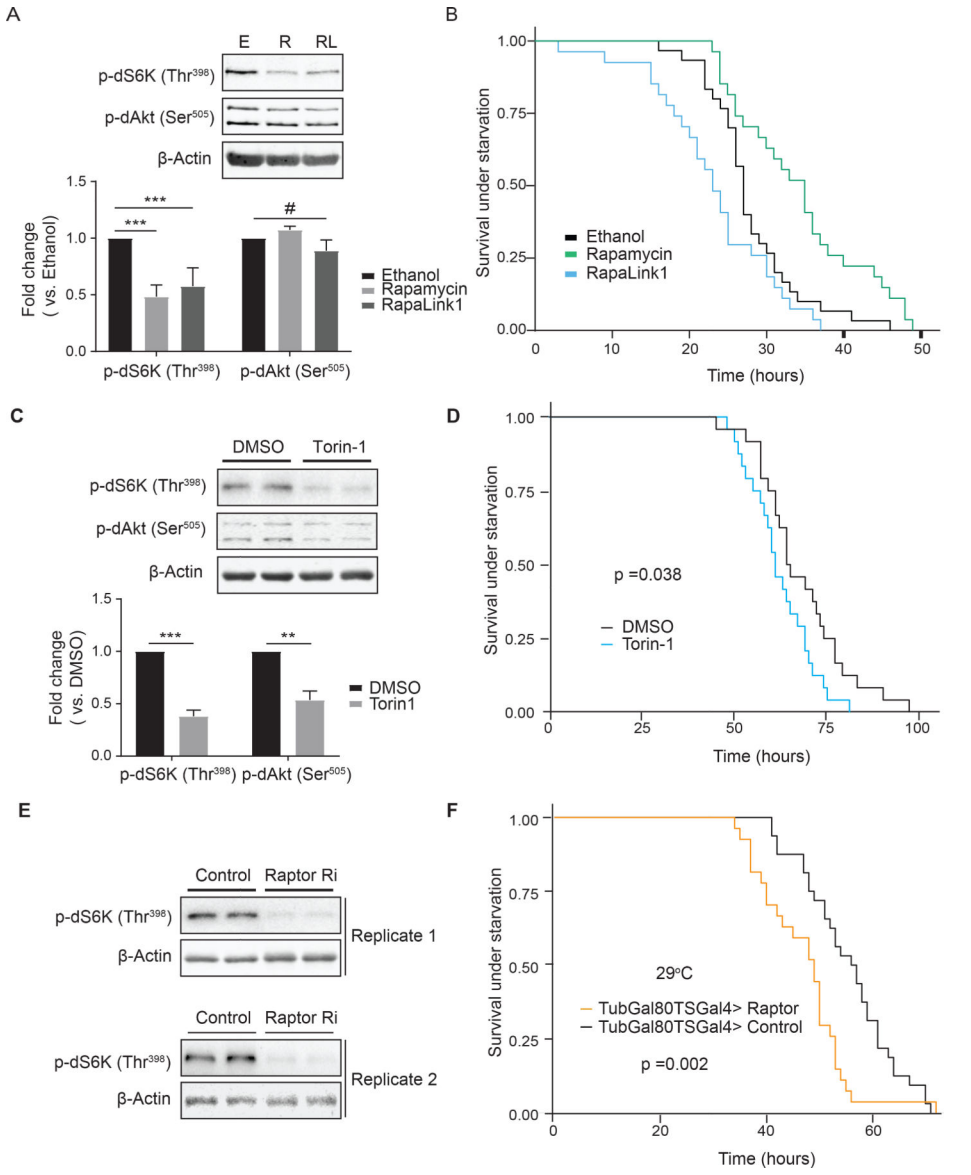

Fig. 5. Complete inhibition of TORC1 reduces starvation resistance in flies.

(A, **B)** Mated adult female flies were fed with ethanol (E), 200uM rapamycin (R) or 6μM RapaLink1 (RL) for 3 d. The heads and thoraxes of 5 flies were subjected to Western blotting for the indicated proteins, which was quantified (A). The results are shown as mean ± SEM from 4 independent experiments (*** $p < 0.005$, # No significant difference, two-tailed student's t-test). Remaining flies were placed into *Drosophila* activity monitor system (DAMS) tubes with 2% agar for continuous monitoring (B). The p-values for rapamycin and RapaLink1 treatments are 0.002 and 0.052 respectively (log-rank test compared to ethanol treatment, n=16 for each group). **(C**, **D)** Mated adult female flies were fed with DMSO or 10uM Torin-1 for 3 d. The heads and thoraxes of 5 flies were subjected to Western blotting for the indicated proteins, which was quantified (C). The results are shown as mean ± SEM from 3 independent experiments (** $p < 0.01$, *** $p < 0.005$, two-tailed student's t-test). The remaining flies were placed into DAMS tubes with 2% agar for continuous monitoring.

Log-rank test was performed (n=16 for each group) (D). **(E, F)** Mated *tubulin*-GAL80 ^{ts}; *tubulin*-GAL4 UAS-Raptor ^{HMS02306} RNAi or control adult female flies were raised at 18^{o}C and shifted to 29^{o}C for 3 d. The heads and thoraxes of 5 females were subjected to Western blotting for the indicated proteins from 2 independent experiments (E). Sixteen females per genotype were placed into DAMs tubes with 2% agar for continuous monitoring. Log-rank test was performed (F).